Vol 4 | Issue 1 | Pages 123-130

Journal of Botany Research
ISSN: 2643-6027

Research Article

DOI: 10.36959/771/569

Contribution of Mitochondrial F_0F_1-ATP Synthase and Adenine Nucleotide Translocator to Induced Thermogenesis in the Appendix of *Sauromatum venosum* Inflorescence

*Hanna Skubatz, PhD**

NeoPro Labs, USA

Abstract

Thermogenesis in the appendix of *Sauromatum venosum* inflorescence can be induced by aspirin, salicylic acid, and 2-6-dihydroxybenzoic acid. The contribution of mitochondrial F_0F_1 ATP synthase, adenine nucleotide translocator, and alternative oxidase to induced thermogenesis in various light and dark regimes was studied. Sections of the appendix of the *Sauromatum* appendix were incubated with each of three inducers under a series of different photoperiods ranging from 6-48 h of dark or light regimes. The effect of mitochondrial inhibitors, oligomycin (F_0F_1 ATP synthase inhibitor), carboxyatractyloside (adenine nucleotide translocator inhibitor), and SHAM (alternative oxidase inhibitor) were used to demonstrate F_0F_1 ATP synthase, adenine nucleotide translocator, and alternative oxidase contribution to temperature rise. Under night/light conditions temperature rose 3 h since light onset and 12 h since darkness onset under various dark to light regimes. Temperature rise was suppressed by 40 µM oligomycin and 40 µM carboxyatractylosid in dark/light and light/dark regimes. Combination of the two inhibitors and an inducer completely suppressed temperature rise. When the appendix sections were treated with 2 mM salicylhydroxamic acid, temperature rise was significantly suppressed only under prolonged light conditions, more than 20 h of light.

Keyword

Adenine nucleotide Translocator, Aspirin, 2,6-dihydroxybenzoic acid, F_0F_1-ATP synthase, Induced thermogenesis, Salicylic acid

Abbreviations

ANT: Adenine nucleotide translocator; AOX: Alternative oxidase; ASA: Aspirin; CV: mitochondrial complex V (F_0F_1 ATP synthase); D/L: Dark/light; 2,6-DHBA: 2,6-dihydroxybenzoic acid; L/D: Light/dark; OM: Oligomycin; OXPHOS: Oxidative phosphorylation; PTP: Permeability transition pore; SA: Salicylic acid; SHAM: Salicylhydroxamic acid

Introduction

Aspirin (ASA), SA, and 2,6-DHBA induce thermogenesis in tissue slices of the *Sauromatum* appendix over a wide range of concentrations [1]. Recently, it has been shown that mitochondrial OXPHOS activity is a prerequisite for this inducible thermogenesis [2]. Suppression of induced thermogenesis was observed when *Sauromatum* appendix tissue slices were treated with a diverse set of inhibitors of the mitochondrial electron transport chain under constant light. Unexpectedly, treatment with 2 mM SHAM did not completely suppress temperature rise. On the other hand, OM (a CV inhibitor) and CATR (an ANT inhibitor) suppressed temperature rise. One possible explanation for the unexpected results is that thermogenesis in the *Sauromatum* appendix is a sum of three heat sources. One source is AOX and two other likely additional heat sources are CV and ANT. The inhibitors affect only mitochondrial functions in the *Sauromatum* appendix tissue because the tissue lacks chloroplasts [3].

F_0F_1-ATP synthase is abundant and organized in two subcomplexes in plant mitochondrial like in other eukaryotes [4,5]. The F_0 subcomplex is composed of several proteins

***Corresponding author:** Hanna Skubatz Ph.D., CEO, NeoPro Labs, 3161 Elliott Ave, Suite 308, Seattle, WA 98121, USA, Tel: 1-206-447-5170

Accepted: February 25, 2021

Published online: February 27, 2021

Citation: Skubatz H (2021) Contribution of Mitochondrial F_0F_1-ATP Synthase and Adenine Nucleotide Translocator to Induced Thermogenesis in the Appendix of *Sauromatum venosum* Inflorescence. J Bot Res 4(1):123-130

including various copies of subunit c (c ring) and subunit b (peripheral stalk). The F_1 subcomplex is composed of three αβ dimers (catalytic site) and a central stalk. The oligomycin sensitivity conferral protein (OSCP) connects the peripheral stalk to the catalytic site [6]. OSCP is necessary for coupling proton translocation to ATP synthesis [7,8].

Plant mitochondrial ANT is one of the most abundant proteins in the inner membrane and it mediates the exchange of mitochondrial ATP^{4-} for cytosolic ADP^{3-} [9,10]. Carboxyatractyloside is a specific inhibitor of plant [11] and human ANT [12]. It blocks ATP transport into mitochondria. ANT mediates proton leak induced by fatty acid in brown-fat mitochondria [12].

F_0F_1-ATP synthase can form various macromolecular complexes. For example, ATP synthasome constitutes ANT, CV, and the phosphate carrier [13,14]. In a different arrangement, ANT, CV, and voltage-dependent anion channel (VDAC) can form a PTP complex [15,16].

In non-thermogenic plants the activity of mitochondrial AOX is high when carbohydrate level is high [17]. Light/dark transitions result in an increase in both dark respiration and AOX activity because of carbohydrates accumulation during photosynthesis [18]. However, under prolong light conditions respiration rate varies among plant species; in some species it can be inhibited and in others stimulated or unchanged [19,20].

The present paper provides evidence that ANT, CV and AOX generate heat in the *Sauromatum* appendix in the presence of the three inducers. Switching between light and darkness changed the intensity of the heat sources and their timing. The D/L regimes generated a temperature peak 3 h since light onset and L/D regimes generated a temperature peak 12 h since light offset. Under various D/L regimes CV and ANT activities generated most of the heat. Under various L/D regimes AOX, CV and ANT contribute to thermogenesis. Only under prolonged light regimes AOX was the major contributor of heat.

Materials and Methods

Materials and chemicals

Antimycin A, carboxyatractyloside, oligomycin, and SHAM were purchased from Sigma Aldrich and dissolved either in ethanol or in DMSO. ASA, SA, and 2,6-DHBA were purchased from Fisher Scientific and dissolved in distilled water to make 2 mM stock solutions.

Plant material

Corms of *Sauromatum vensosum* were kept at 4 °C and the inflorescences were allowed to develop under A normal 15/9 L/D cycle at ambient. When the inflorescence matures the base of the spathe becomes swollen and its color changes to burgundy [21]. These characteristics appear ~3 d prior to thermogenesis (pre D-day stage). At this stage, application of an inducer triggers thermogenesis.

Induction of a thermogenic response

Pre D-day appendices of the *Sauromatum* inflorescences were cut transversely into equal length sections (1-2 cm) and immediately immersed in different concentrations of an inducer solution or in a control solution (buffer solution with no inducer) in a 96 well plate in an environmental chamber (SANYO) under different light and dark regimes at ~20 °C. The inducer solution contained one of the following compounds, SA, ASA, or 2,6-DHBA, and 0.5% Teeen-20 in 20 mM HEPES buffer, pH 7.0 [1].

Treatments under different photoperiods were as follows: 6L:42D, 9L/39D, 12L:36D, 15L/33D, 20L: 28D, 24L:24:D, and 48L:0D. In another set of experiments sections were incubated under different darkness periods: 6D:42L, 9D/38L, 12D:32L, 15D:33L, 20D:28L, 24D:24L and 48D:0L. Each set of experiments was performed with sections from one appendix. Appendix sections were immersed in the solution throughout the experimental period. Data collection started as soon as the appendix sections were placed in a solution.

Temperature data collection

Precision thermocouples (copper/constantan, Omega Engineering, Stamford, CT) were inserted into the appendix sections and the temperature was recorded by a data logger (OMB- DAQ-56, Omega) every 2 min. There were 720 consecutive readings per 24 h. The effect of a treatment on the temperature rise was calculated as the difference in temperature between an inducer and a buffer treated section. Temperature rate was defined as Δ°C/h and was calculated by subtracting the first reading (the first 2 min) from of the first hour (62 min) and dividing by time (60 min). The moving average of temperature rate data was created using Excel software.

Results

Induced thermogenesis response to dark/light transitions in the appendix of the *Sauromatum* inflorescence

Figure 1 shows the timing of induced thermogenesis as a response to the duration of the dark phase in the presence of ASA, SA, and 2,6-DHBA. When the dark phase preceded light onset by 6 h the temperature rose ~23-25 h since darkness onset (the beginning of the experiment) or 17-19 h since light onset (Figure 1, row 1). Two weak temperature peaks were observed after 9-12 h of darkness in the presence of SA and 2,6-DHBA (row 2-3). One peak occurred ~3 h since light onset and a second peak ~26-29 h since darkness onset. The time interval between the peaks was ~12-13h. The weak thermogenic response to inducers under 9 to 12 h of darkness seems to coincide with a shift in the timing of induced thermogenesis. It resembles a phase shift in a rhythm of a circadian clock.

Prolong darkness, more than 12 h, initiated a temperature rise ~3 h since light onset regardless of darkness duration (row 4-5). Under 24 h of darkness, thermogenesis appeared prior to the light onset and therefore the effect of temperature change in environmental chamber on the tissue slices seemed minimal (row 6). It may suggest that the thermogen-

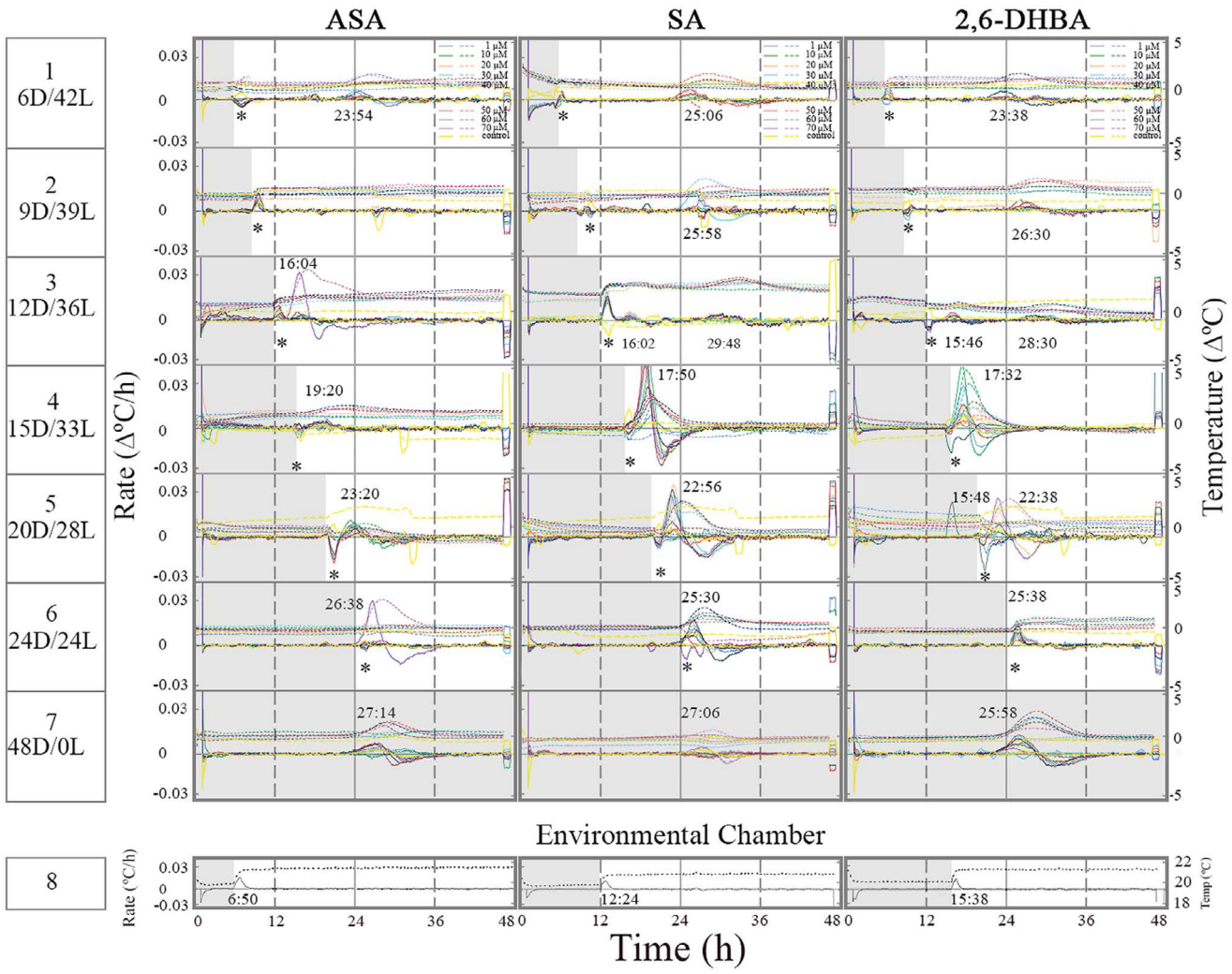

Figure 1: Effect of D/L transitions on induced thermogenesis in the appendix of the *Sauromatum* inflorescence. Each column depicts tissue temperature in the present of one of the inducers (ASA, SA, or 2,6-DHBA) at increasing concentrations (1-70 µM). Data are expressed as temperature values above chamber temperature (dashed lines, right vertical axis) and corresponding temperature rates (solid lines, left vertical axis). The time to reach temperature maximum rate was determined from the start of the experiment. The gray and white areas represent the dark and light phases, respectively. Star symbol depicts the change in temperature due to increase in the environmental chamber temperature when light was switched on. Dark/light transitions depict on the first left column. The spike in temperature at the first h is temperature equilibration in the environmental chamber. Untreated control dash and straight lines (yellow). Each treatment (one row) was carried out with two pre D-day appendices.

ic rhythm shifted under prolong darkness (24 h of darkness). Interestingly, when the environmental chamber light was turned on and the temperature increased (row 8), the temperature of the control tissue slices (untreated) decreased. The temperature of the treated tissue sliced fluctuated either it dropped or went up and in some tissue slices it stayed unchanged. Under constant darkness thermogenesis appeared ~25-27 h since darkness onset (row 7). It may suggest that under constant darkness with no light cue thermogenesis occurred later than 24 h because of a change in a putative circadian clock.

Induced thermogenesis response to light/dark transitions in the appendix of the *Sauromatum* inflorescence

Light/dark transitions caused to lengthen the time to reach a temperature maximum rate, which appeared 12 h since light offset over a wide range of inducer concentrations (Figure 2). As the light phase advanced, the temperature rise appeared 3 h later (row 1 vs. row 2-3). At 20L/28D, temperature rise was low (row 5) and later at 24L/24D it rose again (row 6). Thermogenesis at 20L/28D seems to correspond to a phase shift in a rhythm of a circadian clock under these L/D conditions.

Under 24 h of light, thermogenesis appeared at the end of the dark phase and therefore the effect of temperature change in environmental chamber on the tissue slices was minimal (row 6). It may suggest that the thermogenic rhythm shifted under a 24 h light phase. Under constant light thermogenesis appears ~22-23 h since light onset (row 7). It may suggest that under constant light, thermogenesis occurred earlier than 24 h because of a change in a putative circadian clock.

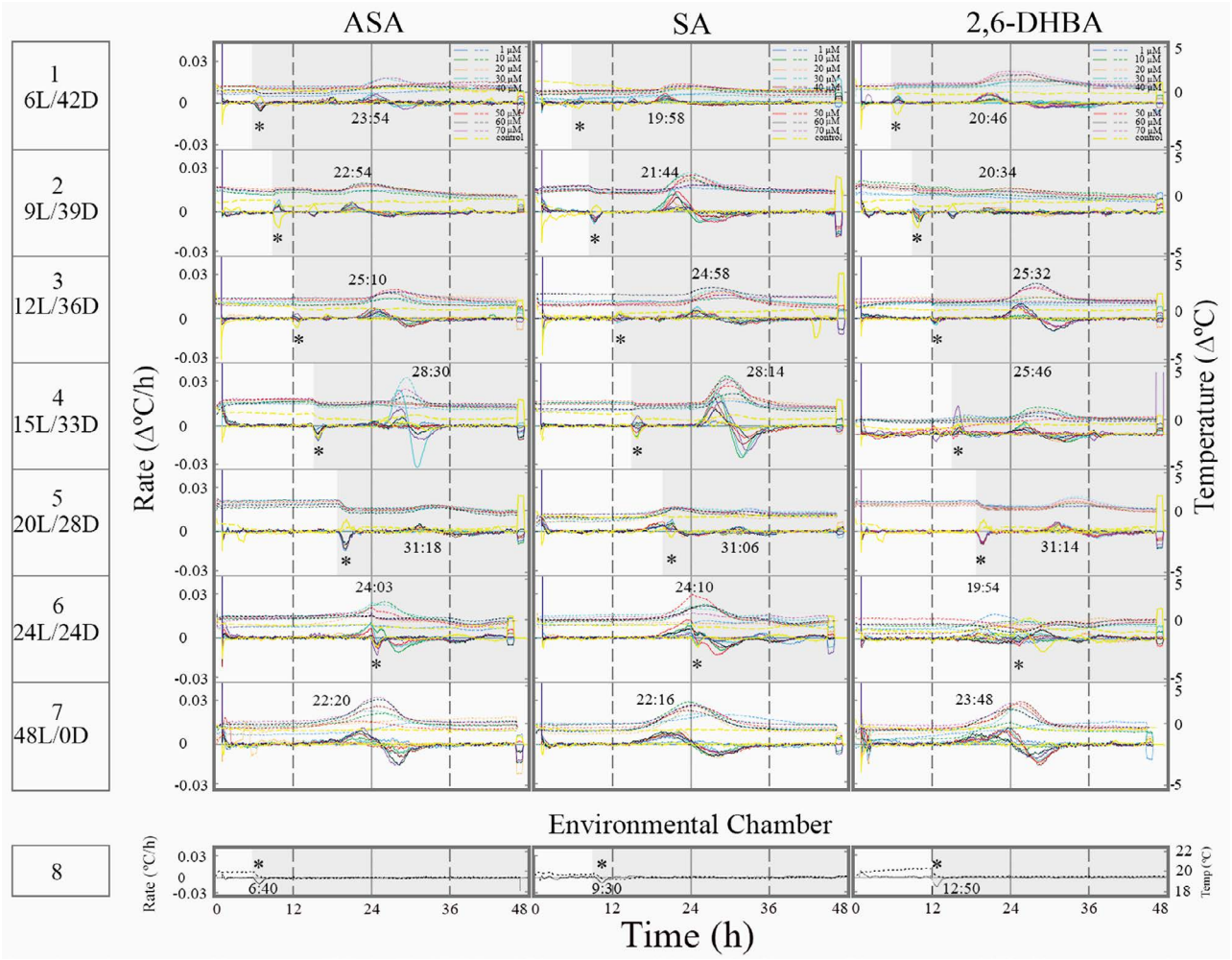

Figure 2: Effect of L/D transitions on induced thermogenesis in the appendix of the *Sauromatum* inflorescence. Legend as described in the legend of Figure 1. Star symbol depicts the change in temperature of tissue slices because of switching off the lights.

Effect of SHAM, oligomycin, and carboxyatractyloside on induced thermogenesis at dark/light regimes in the appendix of the *Sauromatum* inflorescence

Treatment of tissue slices with 2 mM SHAM at three different D/L regimes did not suppress temperature rise in the presence of ASA, SA and 2,6-DHBA (Figure 3, row 1-3). Also, it seems that the temperature rose at darkness prior to light onset in the presence of SHAM suggesting that AOX activity is required for the timing of thermogenesis. In SA-treated tissue slices (row 2) the temperature maximum rate split into 3 peaks because of the change in environmental chamber temperature. In tissue slices treated with1 µM 2,6-DHBA plus SHAM, thermogenesis started at ~9 h since the onset of darkness (row 2). The fact that at 1 µM 2,6-DHBA the temperature rise appeared prior to the temperature rise at higher concentrations may suggest that different heat sources respond differently to 2,6-DHBA. At 1 µM the heat sources appeared in sequence and at higher concentrations the sources were superimposed at the same time.

The effect of OM and CATR on induced thermogenesis was studied at 15D/33L. Oligomycin suppressed some of the temperature rise in the presence of ASA and SA (row 4 vs. row1-3). The timing of temperature rate maximum remained unchanged (3 h since light onset). Induced thermogenesis was completely suppressed in the presence of 2,6-DHBA and OM suggesting that thermogenesis induces by 2,6-DHBA mostly originates from CV. Combination of OM and SHAM did not have any additive effect in the presence of inducers (row 5).

The effect of OM on induced thermogenesis raised the question whether ANT, which can form a complex with CV contributes to thermogenesis in the *Sauromatum* appendix. Treatment with CATR, an ANT inhibitor, also suppressed induced thermogenesis to some degree at unchanged timing (row 6 vs. rows 1-3). It may suggest that the heat comes in equal amounts from two additional sources: genera CV and ANT. Treatment with a combination of SHAM and CATR further suppressed induced thermogenesis at the light phase (row 7 vs. row 6). Temperature rise in the presence of 2,6-DHBA occurred at the end of the dark phase, earlier than in the presence of ASA and SA. It seems that inhibition of ANT increased the activity of AOX in the presence of the three inducers. Treatment with a combination of OM and CATR com-

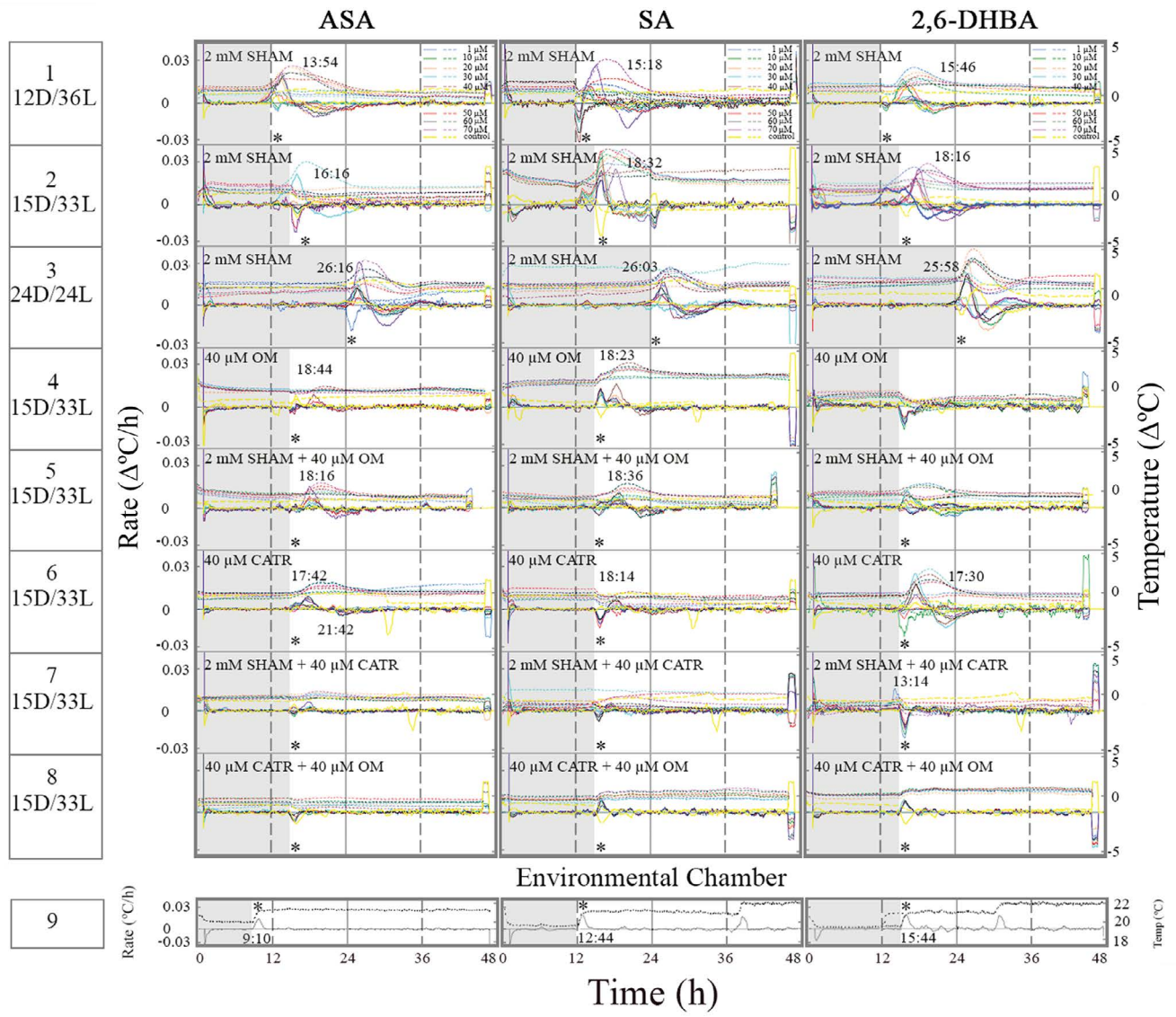

Figure 3: Effect of mitochondrial inhibitors on induced thermogenesis during D/L in the appendix of the *Sauromatum* inflorescence. Legend as described in the legend of Figure 1.

pletely suppressed induced thermogenesis in the presence of the three inducers (row 8). It strongly suggests that CV and ANT generated most of the heat observed under dark/light regimes and AOX was active only when thermogenesis generated by ANT was suppressed. The heat from AOX, CV, and ANT were superimposed upon each other making their detection difficult.

Effect of SHAM, oligomycin, and carboxyatractyloside on induced thermogenesis at light/dark regimes in the appendix of the *Sauromatum* inflorescence

Treatment of tissue slices with 2 mM SHAM at two different L/D regimes did not suppress temperature rise in the presence of ASA, SA and 2,6-DHBA (Figure 4, row 1-2). Treatment with a combination of AA and SHAM in the presence of an inducer suppressed induced thermogenesis (row 3). It strongly suggests that *in vivo* SHAM ineffectiveness is not due to a permeability barrier. Treatment with AA alone did not suppress induced thermogenesis suggesting that AOX is inactive under 15L/28D (row 3 vs. row 4). When AOX activity was low, at 15L/28D, OM (row 7) and CATR (row 8) suppressed induced thermogenesis. SHAM at 2 mM suppressed induced thermogenesis only under 15L/28D suggesting that prolonged light phase activates AOX (rows 5-6). ASA seems to be less effective in activation of AOX under 24L/24D (row 6).

Discussion

This is the first study that shows the involvement of CV and ANT in the thermogenic response to inducers in the *Sauromatum* appendix. It also shows that AOX, CV and ANT activities are under and D/L control. Further studies are required for providing more detail information on the control mechanism.

Mitochondrial alternative oxidase

The results of this study suggest that AOX that is abundant in the mitochondria of the *Sauromatum* appendix [22] is not

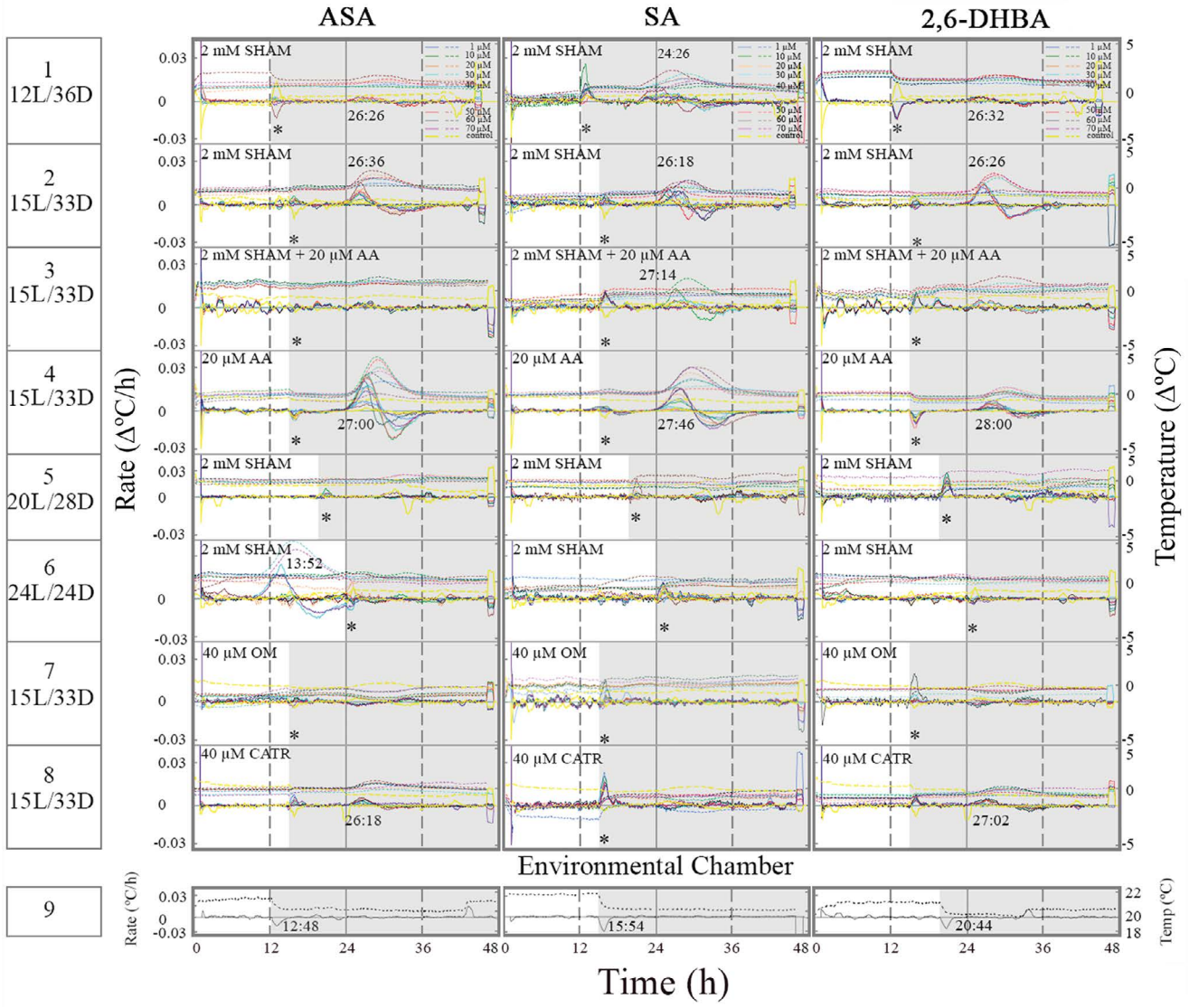

Figure 4: Effect of mitochondrial inhibitors on induced thermogenesis during L/D transitions in the appendix of the *Sauromatum* inflorescence. Legend as described in the legend of Figure 2.

fully active under various darkness and light regimes. Furthermore, AOX is not the only source of heat and mitochondrial CV and ANT also contribute to temperature rise in this appendix. The mechanism that control AOX activity under light and darkness in the absence of chloroplasts is unclear. One possible explanation is that the dimerization of AOX under different L/D regimes controls its activity [18,23].

Proton leakage through mitochondrial F_oF_1 ATP synthase

In humans, CV can leak via the c-ring that is made up of 8-15 c subunits and it serves as a carrier of protons [24]. Mutation in an arginine moiety in the c-ring leads to proton leakage and decreases ATP synthesis [25]. F1Fo ATP synthase can also be involved in PTP activity that leads to inner membrane depolarization [15]. This leakage can be transformed into an energy-dissipating process. In plants the presence of the c-ring and PTP activity has been described [26]. In the *Sauromatum* appendix tissue the ratio of ATP/ADP is low (~1.5) during thermogenesis and it is possible that CV leakage in addition to AOX activity makes ATP production inefficient [27]. The activity and properties of CV in the *Sauromatum* appendix and in other thermogenic plants have not been studied.

It has been suggested that plant mitochondria can regulate their CV under different L/D transitions [28]. 14-3-3 protein that down regulates chloroplast ATP synthase during dark adaption was found in the mitochondrial inner membrane. It has to be determined whether this protein is involved in the regulation of CV under different L/D and D/L regimes in the *Sauromatum* appendix.

Proton leakage through mitochondrial adenine nucleotide translocator

In humans, adenine nucleotide translocator has uncoupling properties that can account for up to 50% of basal mitochondrial membrane proton conductance [29,30]. It has been suggested that leakage through ANT can be activated by fatty acids [31,32]. This uncoupling can be transformed into an en-

ergy-dissipating process and it also can decrease the efficiency of ATP synthesis. In plants, ANT is present several subcellular organelles, e.g., chloroplast, peroxisomes, and mitochondria [9,33]. It has been isolated and characterized [34] but its involvement in thermogenicity has not been examined. The activity and properties of ANT in the *Sauromatum* appendix and in other thermogenic plants have not been studied.

Coupling between thermogenesis and a putative clock(s)

The data in the present article suggest that L/D and D/L transitions are coupled to a timing mechanism. The timing of thermogenesis varies between light and dark onset in the presence of ASA, SA, and 2,6-DHBA. The timing of thermogenesis is ~3h after the darkness onset and ~12 h after light onset. It is known that circadian system is temperature resistant and maintains approximately 24 h mechanism it has also been shown despite ambient temperature changes [35]. However, it has been shown that mammalian body temperature can have a weak synchronization effect on the circadian system [36-38]. Whether the mitochondria possess a clock activity is still an open question in mammals [39] as well as in plants and especially in thermogenic plants.

It has well established that mitochondrial network oscillates [40-42]. Mitochondrial fission-fusion display diurnal changes aligned to L/D cycles [43]. Mitochondrial fusion and fission contribute to maintenance of mitochondrial function [44,45]. In the *Sauromatum* appendix tissue the mitochondria are fusing and divided during thermogenesis [3] and it raises the question whether the morphological changes are the reason for heat production by AOX, CV and ANT.

Conclusions

1) Existence of three, superimposed up on each other, components of induced thermogenesis in the appendix of the *Sauromatum venosum* inflorescence: alternative oxidse, F_1F_0 ATP synthase, and adenine nucleotide translocator.
2) Alternative oxidase activity is high only under prolong light conditions.
3) Induced thermogenesis is low during a shift in timing.
4) Contribution of F_0F_1 ATP synthase, adenine nucleotide translocator to temperature rise was higher under dark/light regimes than under light/dark regimes.
5) A time-keeping system is involved in induced thermogenesis and is dependent on the duration of darkness and light.

Funding Sources

This research did not receive any grant from funding agencies in the public, commercial, or not-for-profit sectors.

Conflicts of Interest

The author declares no conflict interest.

References

1. Skubatz H (2014) Thermoregulation in the appendix of the *Sauromatum guttatum* inflorescence. Bot Stud 55: 68-81.
2. Skubatz H (2020) Mitochondrial oxidative phosphorylation controls SA-induced thermogenesis in the appendix of *Sauromatum guttatum*. Asian J Research Bot 3: 28-37.
3. Skubatz H, Kunkel DD, Meeuse BJD (1993) Ultrastructural changes in the appendix of the *Sauromatum guttatum* inflorescence during anthesis. Sex Plant Reprod 6: 153-170.
4. Velours J, Arselin G (2000) The *Saccharomyces cerevisiae* ATP synthase. J Bioenerg Biomem 32: 383-390.
5. Zancani M, Braidot E, Filippi A, et al. (2020) Structural and functional properties of plant mitochondrial F-ATP synthase. Mitochondrion 53: 178-193.
6. Joshi S, Cao GJ, Nath C, et al. (1997) Oligomycin sensitivity conferring protein (OSCP) of bovine heart mitochondrial ATP synthase: high-affinity OSCP-F_O interactions require a local α-helix at the C-terminal end of the subunit. Biochemistry 36: 10936-10943.
7. Devenish RJ, Prescott M, Boyle GM, et al. (2000) The oligomycin axis of mitochondrial ATP synthase: OSCP and the proton channel. J Bioenerg Biomem 32: 507-515.
8. Giorgio V, Fogolari F, Lippe G, et al. (2019) OSCP subunit of mitochondrial ATP synthase: role in regulation of enzyme function and of its transition to a pore. British J Pharmacol 176: 4247-4257.
9. Haferkamp I, Fernie AR, Neuhaus HE (2011) Adenine nucleotide transport in plants: much more than a mitochondrial issue. Trends Plant Sci 16: 507-515.
10. Klingenberg M (2008) The ADP and ATP transport in mitochondria and its carrier. Biochim Biophys Acta 1778: 1978-2021.
11. Lima MS, Denslow ND (1979) The effect of atractyloside and carboxyatractyloside on adenine nucleotide translocation in mitochondria of Vigna sinensis (L.) Savi cv. seridó. Arch Biochem Biophys 193: 368-372.
12. Shabalina IG, Kramarova TV, Nedergaard J, et al. (2006) Carboxyatractyloside effects on brown-fat mitochondria imply that the adenine nucleotide translocator isoforms ANT1 and ANT2 may be responsible for basal and fatty-acid-induced uncoupling respectively. Biochem J 399: 405-414.
13. Chen C, Ko Y, Delannoy M, et al. (2004) Mitochondrial ATP synthasome: Three-dimensional structure by electron microscopy of the ATP synthase in complex formation with carriers for Pi and ADP/ATP. J Biol Chem 279: 31761-31768.
14. Seelert H, Dencher NA (2011) ATP synthase super assemblies in animals and plants: Two or more are better. Biochim Biophys Acta 1807: 1185-1197.
15. Carraro M, Checchetto V, Szabó I, et al. (2019) F-ATP synthase and the permeability transition pore: fewer doubts, more certainties. FEBS Lett 593: 1542-1553.
16. Kusano T, Tateda C, Berberich T, et al. (2009) Voltage-dependent anion channels: Their roles in plant defense and cell death. Plant Cell Rep 28: 1301-1308.
17. Azcón-Bieto J, Lambers H, Day DA (1983) Effect of photosynthesis and carbohydrate status on respiratory rates and the involvement of the alternative pathway in leaf respiration. Plant Physiol 72: 598-603.
18. Feng HQ, Li HY, Li X, et al. (2007) The flexible interrelation between AOX respiratory pathway and photosynthesis in rice leaves. Plant Physiol Biochem 45: 228-235.

19. Zhang DW, Xu F, Zhang ZW, et al. (2010) Effects of light on cyanide-resistant respiration and alternative oxidase function in *Arabidopsis* seedlings. Plant Cell Environ 33: 2121-2131.

20. Xu F, Yuan S, Lin HH (2011) Response of mitochondrial alternative oxidase (AOX) to light signals. Plant Signal Behav 6: 55-58.

21. Meeuse BJD (1966) The voodoo lily. Sci Am 215: 80-89.

22. Elthon TE, Nickels R, McIntosh L (1989) Mitochondrial events during development of thermogenesis in *Sauromatum guttatum* (Schott). Planta 180: 82-89.

23. Day DA, Wiskich JT (1995) Regulation of alternative oxidase activity in higher plants. J Bioenerg Biomem 27: 379-385.

24. Alavian KN, Beutner G, Lazrove E, et al. (2014) An uncoupling channel within the c-subunit ring of the F_1F_OATP synthase is the mitochondrial permeability transition pore. Proc Nat Acad Sci USA 111: 10580-10585.

25. Kubo S, Niina T, Takada S (2020) Molecular dynamics simulation of proton-transfer coupled rotations in ATP synthase F_O motor. Sci Rep10: 8225.

26. Zancani M, Casolo V, Petrussa E, et al. (2015) The permeability transition in plant mitochondria: The missing link. Front Plant Sci 6: 1120.

27. Skubatz H, Hardin CD, Wiseman B, et al. (1992) The energetic state of the thermogenic appendix of the voodoo lily inflorescence. A ^{31}P- NMR study. Biochim Biophys Acta 1100: 98-103.

28. Bunney TD, van Walraven HS, de Boer AH (2001) 14-3-3 protein is a regulator of the mitochondrial and chloroplast ATP synthase. Proc Nat Acad Sci USA 98: 4249-4254.

29. Halestrap AP (2004) Dual role for the ADP/ATP translocator? Nature 430: 984.

30. Brand MD, Pakay JL, Ocloo A, et al. (2005) The basal proton conductance of mitochondria depends on adenine nucleotide translocase content. Biochem J 392: 353-362.

31. Andreyev AY, Bondareva TO, Dedukhova VI, et al. (1989) The ATP/ADP-antiporter is involved in the uncoupling effect of fatty acids on mitochondria. J Biol Inorg Chem 182: 585-592.

32. Bertholet AM, Chouchani ET, Kazak L, et al. (2019) H+ transport is an integral function of the mitochondrial ADP/ATP carrier. Nature 571: 515-520.

33. Millar AH, Heazlewood JL (2003) Genomic and proteomic analysis of mitochondrial carrier proteins in Arabidopsis. Plant Physiol 131: 443-453.

34. Spagnoletta A, Santis AD, Palmieri F, et al. (2002) Purification and characterization of the reconstitutively active adenine nucleotide carrier from mitochondria of Jerusalem artichoke (Helianthus tuberosus L.) tubers. J Bioenerg Biomem 34: 465-472.

35. Pittendrigh CS (1954) On temperature independence in the clock system controlling emergence time in Drosophila. Proc Nat Acad Sci USA 40: 1018-1029.

36. Brown SA, Zumbrunn G, Fleury-Olela F, et al. (2002) Rhythms of mammalian body temperature can sustain peripheral circadian clocks. Curr Biol 12: 1574-1583.

37. Refinetti R (2010) Entrainment of circadian rhythm by ambient temperature cycles in mice. J Biol Rhythms 25: 247-256.

38. Ki Y, Ri H, Lee H, et al. (2015) Warming up your tick-tock: temperature-dependent regulation of circadian clocks. Neuroscientist 21: 503-518.

39. Aon MA, O'Rourke CB (2008) Is there a mitochondrial clock? In: Lloyd D, Rossi EL, Ultradian Rhythms from Molecules to Mind. 129-144.

40. Bass J, Takahashi JS (2010) Circadian integration of metabolism and energetics. Science 330: 1349-1354.

41. Buhr ED, Yoo SH, Takahashi JS (2010) Temperature as a universal resetting cue for mammalian circadian oscillators. Science 330: 379-385.

42. Aguilar-López BA, Moreno-Altamirano MMB, Dockrell HM, et al. (2020) Mitochondria: An integrative hub coordinating circadian rhythms, metabolism, the microbiome, and immunity. Front Cell Dev Biol 8: 51.

43. Schmitt K, Grimm A, Dallmann R, et al. (2018) Circadian control of DRP1 activity regulates mitochondrial dynamics and bioenergetics. Cell Met 27: 657-666.e5.

44. Westermann B (2010) Mitochondrial fusion and fission in cell life and death. Nature Rev Mol Cell Biol 11: 872-884.

45. Ezagouri S, Asher G (2018) Circadian control of mitochondrial dynamics and functions. Curr Opin Physiol 5: 25-29.

DOI: 10.36959/771/569